Glucocorticoid receptor knockdown and adult hippocampal neurogenesis

Hooijdonk, L.W.A. van

4

GLUCOCORTICOID RECEPTOR REGULATES FUNCTIONAL INTEGRATION OF NEWBORN NEURONS IN THE HIPPOCAMPUS

L.W.A. van Hooijdonk[1*], C.P. Fitzsimons[1*], T.G. Schouten[1], T.F. Dijkmans[1], I.M.C. Bakker[1], J. Shi[1], F.J. Verbeek[3], E.R. de Kloet[1], H. Karst[2], M. Joels[2], M.S. Oitzl[1] and E. Vreugdenhil[1].

*Both authors contributed equally

This paper, in combination with the paper of CHAPTER 5 was submitted to Neuron

ABSTRACT

Stress is a major factor affecting adult hippocampal neurogenesis. However, the role of one of the major mediators of the stress response in neuronal progenitor cells (NPCs), the glucocorticoid receptor (GR), is unknown. Here, we show that specific GR knockdown in NPCs accelerated neuronal differentiation and migration. Strikingly, GR knockdown led to mis-positioning of adult newborn neurons, to altered dendritic arborization, to higher numbers of mature mushroom and thin spines and to larger mossy fiber boutons. In line with increased numbers of synaptic contacts, adult newborn neurons with GR knockdown exhibit increased mEPSC frequencies. Together, our data show a key role for GR expression levels in the appropriate formation of hippocampal neo-circuits.

INTRODUCTION

In the adult brain, neuronal progenitor cells (NPCs) exist in the sub-granular cell layer of the dentate gyrus, a subfield of the hippocampus that is involved in learning and memory formation. NPCs proliferate, and a subpopulation of these migrate and differentiate into granule neurons that are integrated into functional hippocampal networks (reviewed in [62]). Together, this process takes approximately 4 weeks and is known as adult hippocampal neurogenesis. Previous pharmacological and physical [280;448] and recent genetic manipulations [98;406;449] aiming at blockade of neurogenesis have provided convincing evidence for a role of neurogenesis in hippocampus-dependent memory formation.

Among the most profound and best-studied regulators of neurogenesis are glucocorticoids (GC), which are one of the main mediators of the stress response. In the brain, GCs have profound effects on hippocampal networks that underlie behavioural adaption to stress. Prolonged periods of elevated GC levels, induced by e.g. chronic stress, have been associated with alterations in neuronal plasticity [371] and decreased levels of neurogenesis [139;244;450].

GCs exert their effect by binding to two types of receptors i.e. glucocorticoid receptors (GR) and the mineralocorticoid receptor (MR) [14]. Despite the wealth of information on the effect of stress and circulating GC levels on neurogenesis, very little is known on the role of GR and MR in individual NPCs. GRs are known to be expressed in NPCs but the MR is not [56;57]. Two recent studies have suggested that tight GR regulation in NPCs is necessary for proper neurogenesis. Firstly, NPCs contain specialized retrograde transport mechanisms for GR translocation to the nucleus [67]. Secondly, neuron-specific miR-124, a non-coding small RNA molecule regulating proper neuronal differentiation of NPCs *in vitro* and *in vivo* [60;61], down-regulates GR protein levels [59]. Yet, how GR protein levels directly regulate adult-born NPC function is unknown.

To study the *in vivo* role of the GR in NPCs of the sub-granular layer of the DG requires an experimental approach that is not based on traditional pharmacological or genetic manipulations of the GR. Therefore, we used previously characterized lentivirus-based vectors that preferentially transduce a population of DCX+ neuronal progenitor cells and immature dentate granule neurons in the DG (further referred to as NPCs) [109;451] (see also CHAPTER 3). *In vitro*, lentivirus-based vectors containing shRNAs directed against the GR (pm-shGR) were found to gain more than 70% GR protein knockdown (Van Hooijdonk et al., unpublished data (CHAPTER 2)). Using this technique for shRNA transgenesis to knockdown GR protein expression, we found that GR knockdown accelerates neuronal differentiation of NPCs. Moreover, GR knockdown induced aberrant positioning of adult newborn granule neurons in the outer layers of the DG, a higher number of cells with complex dendritic trees and a higher abundance of thin / mushroom-shaped mature spines at the cost of more immature stubby-shaped ones. Strikingly, this aberrant cellular phenotype was associated with enhanced basal neuronal excitability as measured by mEPSC frequencies.

MATERIALS AND METHODS

Animals

Male BALB/c mice (6 weeks, Janvier Bioservices, Genest st Isle, France) were individually housed for one week in filtertop cages before stereotactic surgery. The mice had free access to food and water and were kept under a 12 hour dark/light cycle (lights on at 8.00 hrs) in a temperature (20°C) and humidity controlled room. Experiments were performed between 8.00 and 13.00 hrs. All experiments were approved by the committee on Animal Health and Care from the Leiden University, The Netherlands and the Netherlands ministry of VROM and were performed in strict compliance with the European Union recommendations for the care and use of laboratory animals.

Short hairpin (shRNA) constructs

Perfect match (pm) and two nucleotide mismatch (mm) control short hairpin RNA (shRNA) expression vector and mismatch (mm) control directed against the consensus sequence of mouse, rat and human GR were designed according to the described criteria [373;374]. The sequence for shRNA against mouse GR (NM_008173) was GATCCCCGAAAGCATTGCAAACCTCATTCAAGAGATGAGGTTTGCAATGCTTTCTTTTGGAAA for the pm, and GATCCCCGACAGCATTGCACACCTCATTCAAGAGATGAGGTGTGCAATGCTGTCTTTTGCAAA for the mm control (mismatch positions underlined). The sense and antisense oligonucleotides were annealed and cloned in *BglII* and *HindIII* sites of p-super vector (The Netherlands Cancer Institute, Amsterdam, The Netherlands). Insertion of the oligonucleotides was confirmed by sequencing. The knockdown of the GR by pm-shGR was confirmed by Western Blot in rat PC12 cells and functionally tested in N1E-115 mouse neuroblastoma cells by using a Dual Luciferase (Promega Corp. Madison, WI)- based GC response element reporter gene assay as previously described (see CHAPTER 2).

Lentiviral vectors

P-super vector derived pm-shGR and corresponding mm-shGR constructs were subcloned into a lentiviral vector downstream of the H1 promotor. The lentiviral vector also contained EGFP downstream of the CMV promoter. These replication incompetent and self-inactivating Advanced Generation Lentiviral vectors were produced and titrated as previously described [67] (see CHAPTER 3). Titers of both viruses were comparable and ranged between $1x10^8$ and $1x10^9$ transducing U/ml. Virus suspensions were stored at -80°C until use and were briefly centrifuged and kept on ice immediately before injection.

Stereotactic surgery

Stereotactic injections were performed in the morning, following previously described methods [451] (see CHAPTER 3). For all experiments, (LV-) pm-shGR or -mm-shGR constructs (titers ranged between $1x10^8$ and $1x10^9$ transducing U/ml) were injected bilaterally into the hilus of the DG (AP:

-2.00 mm, ML: +/-1.50 mm, DV: -1.90 mm, relative to Bregma). After surgery, animals were placed under a heating lamp until awakening and checked upon daily. For immunocytochemical experiments a group of 40 mice (N=20 for pm-shGR and N=20 for mm-shGR) was stereotactically injected and sacrificed one week post injection (N=10 for pm-shGR and N=10 for mm-shGR) or five weeks post injection (N=10 for pm-shGR and N=10 for mm-shGR). The results at the five week time point for neuronal makers and GFP positioning were confirmed in the mice that underwent context and cue fear conditioning- (see CHAPTER 5). For electrophysiological experiments, 20 mice were stereotactically injected and sacrificed five weeks later (N= 10 pm-shGR and N= 10 mm-shGR). In all experiments, mice were only included for analysis based upon post-mortum histological evidence of an appropriately targeted micro-injection as visualized by GFP expression in SGZ. Animals with low (<100 GFP+ cells per section), absent or mis-positioned GFP expression were excluded from the experiment and further assessment.

Tissue preparation

For the immunohistochemical experiments, one to five weeks post injection (PI), mice were sacrificed and brains were fixated by transcardial perfusion and processed as described previously [451]. Serial, coronal sections of 20 um thickness, were obtained using a cryostat (Leica CM 1900). All brain sections containing the hippocampus were collected either free-floating in eppendorf tubes containing anti-freeze, or thaw-mounted on SuperFrost object glasses. Superfrost slides were stored at -80°C till further use, whereas free floating sections were stored at -20°C.

For the electrophysiology experiment, 5 week PI, mice at rest were sacrificed by decapitation (one mouse per day, between 9.00 and 9.30 am, when circulating levels of plasma corticosterone are low) Acute hippocampal slices (350 μM thick) for the electrophysiology recordings were made with a vibratome (model VT1000S; Leica, Germany) as described before [452] [30]. Hippocampal slices were stored at room temperature until recordings (for at least 1 h).

Immunohistochemistry

Immunofluorescent double and triple labelling staining procedures were performed following a standard procedure with thaw-mounted sections, and free floating as described [381;451] (see CHAPTER 3). Primary antibodies were from: Santa Cruz Biotechnology, Inc; Heidelberg, Germany (Doublecortin (C-18), used 1:200, Ki67 (M-19), used 1:100; GFAP, mouse monoclonal, used 1:1000); Chemicon-Millipore International BV, Amsterdam, The Netherlands (NeuN (A60), mouse monoclonal, used 1:200; GFP, mouse monoclonal, used 1:200), BD Biosciences, Breda, The Netherlands (Nestin, mouse monoclonal (556309), used 1:200), Abcam (Glucocorticoid receptor, (BuGR2), mouse monoclonal, used 1:500) or Molecular Probes/Invitrogen, Breda, The Netherlands (GFP, chicken polyclonal, used 1:500).

Electrophysiology

In acute hippocampal slices, GFP+ granule cells of both pm- and mm- shGR treatment groups and GFP- cells of both treatment groups were assessed for their physiological properties. Using patch

clamp techniques, spontaneous miniature excitatory postsynaptic currents (mEPSCs) were recorded as a measure of the resting membrane properties of newborn cells. Recordings of mEPSCs were performed as previously described [30]. All values shown in the results section are the average ± SEM of the data. Statistical analysis between control and a single treatment on a given group of cells was carried out using a Student's *t*-test (paired when applicable). If more than two conditions were investigated on a given set of cells, we applied a general linear model for repeated measures (within-subjects contrast). Comparison of several conditions between sets of cells was performed with ANOVA, followed by *post hoc* multiple comparisons of the mean (Tukey). In all cases, $P < 0.05$ indicated significance.

Histological analyses and confocal microscopy

Quantification of EGFP+ cells and quantitative analysis of different classes of neuronal cells in the hippocampus of treated animals were performed using the optical fractionator sampling method, as described by Encinas and Enikolopov [81]. Briefly, every tenth hippocampal section was collected starting at the DG following the fractionator scheme, to ensure that each slice is 200 nm apart from the next slice within each collected set of approximately 11 slices [67;451]. For quantification of EGFP+ cells, three sets of slices from at least three independently injected animals from each experimental group were used. Sections surrounding the injection site were routinely discarded. For quantitative analysis of neuronal cell-types other three sets of slices from at least three independently injected animals from each experimental group were used. Confocal images were acquired using a Nikon C1si Spectral confocal microscope, as described [67]. Expression of markers and cell-localization analyses were done counting more than 50 EGFP+ cells per animal. Co-localization was assessed through the entire z-axis of each cell, using an optical slice of 0.3–0.6 µm. Morphology was analyzed from three-dimensional reconstructions of series of sequential confocal images taken at 0.3–0.6 µm intervals in EGFP+ cells.

Image analysis

For EGFP+ cell-localization analyses within the DG or CA1 sub-fields, maximum intensity z-axis projections of series of sequential confocal images were constructed using ImageJ, as described [67]. Using these projections, EGFP+ cells were automatically identified and counted using Cell Profiler (http://www.cellprofiler.org) [414]. This procedure was validated by comparison to manual counting performed by an experienced operator using the optical fractionator method sampling scheme and unbiased stereology estimation of cell numbers as described by West and co-workers [415]. The "pipeline" used to automate cell counting was composed of the following Cell Profiler's modules, in the specified order: LoadSingleImage, ColorToGray, CorrectIllumination_Calculate, CorrectIllumination_Apply, IdentifyPrimAutomatic. By using this pipeline we routinely found a strong correlation between the manual unbiased stereology method and the automated procedure (r=0.985, Pearson's correlation test performed with GraphPad Prism 4, GraphPad Software, Inc., La Jolla, CA). EGFP+ cells were individually pseudo-coloured to facilitated visualization and cell-localization maps were generated using Cell Profiler. Subsequently, based on

a previously described manual method to study granule cell location within the GCL [416] the GCL was subdivided in four 2-cell-body-wide sub-layers using ImageJ (http://rsb.info.nih.gov/ij/) to generate a superimposed grid, guided by Hoechst 33342 staining of cell nucleus. These sub-layers were denominated: sub-granular zone (SGZ) and granule cell layer (GCL) 1 to 3, as described by others [94;278;368]. Then, the pseudo-coloured cell-localization maps generated with Cell Profiler were used to manually assign and count individual EGFP+ cells to the 4 sub-layers of the GCL of the DG. In all cases, EGFP+ cells present in the apex of the DG were excluded from the analyses. A similar procedure was used in experiments comprising EGFP+ cells in CA1.

GR knockdown measurements

Confocal images were analyzed by an operator blind to the treatment, using *ImageJ* 1.40 software for *Windows* (an open source public domain developed by NIH, USA). Clear-shaped and non-overlapping $EGFP^+$ cells in the granule cell layer of the DG of either perfect match- or mismatch shRNA groups were selected by using *"free hand selection"* mode, guided by Hoechst staining. Sections surrounding injection sites were discarded. The intensity of EGFP+ and mouse-anti-GR-Alexa 594 immuno-labelling in these cells was measured by using Region of Interest (ROI) manager program. The degree of GR knockdown at protein level was estimated by normalizing expression levels in EGFP+ cells within the GCL and sub-granular zone (SGZ) to expression levels in equal numbers of GR+ CA1 neurons within the same hippocampus slice, which were not targeted by the lentivirus delivered to the hilar region.

Quantification of different cell-type markers

EGFP+ cells were automatically identified and counted using Cell Profiler from z-projected confocal images. From the same images, cells positive for each individual co-stained marker were also automatically identified and counted with Cell Profiler using the corresponding confocal channel. Cells positive for each marker analyzed were expressed as percentage of total EGFP+ cells per layer. All image analyses procedures were performed in hippocampal sections from at least three independently injected animals as described above. In all cases, image analyses were performed by an operator blind to the treatment.

Quantification of GFP+ cell distribution among different DG sub-layers

For each DG sub-layer, the number of GFP+ cells were counted –blind to treatment- using Image J *Cell counter* and *ROI Manager* program, respectively. Hoechst/GFP+ cells were counted separately for each DG sub-layer according to the following steps. At first, the DG in the photo was rotated to the horizontal or vertical position. After the rotation, the DG was divided by grids. Grids' size was decided by blades' width (only including dense area), which was fitted by 6 grids (2 grids for one layer: the GCL 1, 2&3). The blades' width is not the same everywhere. Thus an average size of grids was chosen for each picture. The neurons outside the GCL1 but next to it (less than 2 grids distance) were counted as SGZ neurons. Then GFP+ cells were counted over all DG sub-layers.

Later same procedure was followed for quantification of Hoechst/GFP/DCX+ and Hoechst/GFP/NeuN+ neurons.

Dendrite tracing and three-dimensional reconstructions.

Three-dimensional reconstructions of dendritic arbors was performed as described previously [451], using TDR3D software package (http://bioimaging.liacs.nl/tdr3dbase.html), and using a simulated fluorescence process-based algorithm [418]. Series of confocal images of EGFP+ neurons were taken at 0.3–0.6 µm intervals from at least three independently injected animals. All cells used for morphological analyses were positive for the neuronal marker NeuN.

Sholl analysis

Three-dimensional reconstruction of the entire dendritic processes of EGFP+ neurons was made from Z-series stacks of confocal images as described above. All EGFP+ dentate granule cells with largely intact dendritic trees were analyzed for total dendritic length and branch number. Measurements did not include corrections for inclinations of dendritic process and therefore should be considered to represent projected lengths [368]. Sholl analysis for dendritic complexity was carried out using the Sholl Analysis Plugin for ImageJ (http://www-biology.ucsd.edu/labs/ghosh/software/ShollAnalysis_class). Data shown were from a 22 individual EGFP+ dentate granule cells from at least 4 animals per experimental group.

Dendritic spine three-dimensional reconstructions and shape classifications.

Three-dimensional reconstruction of dendritic segments was done from Z-stacks of confocal images series of 100-200 confocal planes taken at 0.1 µm intervals using a 63x oil immersion objective. The confocal stacks were then deconvolved with Huygens Deconvolution Software (Scientific Volume Imaging b.v, Hilversum, the Netherlands). Spine density reconstructions and analysis were performed by automated three dimensional detection and shape classification based on a Rayburst sampling algorithm [453] using NeuronStudio software (http://www.mssm.edu/cnic/tools-ns.html).

Confocal analysis of mossy fiber boutons.

Mossy fiber boutons in the CA3 area were analyzed as described by others [102]. Z-stacks of confocal images series of 100-200 confocal planes were acquired at 0.75 µm intervals with 40X oil lens (numerical aperture, 1.3; Nikon) and a digital zoom of 6. Confocal stacks were then deconvolved Huygens Deconvolution Software.

Statistical analysis

All comparisons of GR knockdown animals with control animals were statistically tested using unpaired Student's t-test. When more than two groups were compared we used a one-way ANOVA test with Tukey's post test if $P<0.05$, as described by van Hooijdonk et al [451]. All values

shown in the results section are the average ± SEM of the data. In all cases, $P < 0.05$ indicated significance.

RESULTS

GR knockdown *in vivo*

To knockdown the GR in NPC and their neurogenic progeny *in vivo*, lentivirus suspensions were delivered to the DG of the adult mouse hippocampus by stereotactic injections to the hilar region. Immunohistochemistry to detect the GR confirmed effective knockdown in LV-pm-shGR (further referred to as GR knockdown) EGFP+ cells, while LV-mm-shGR (further referred to as control) was ineffective on GR expression (Figure 4.1 B-G). After semi-quantification, we observed a significant GR knockdown of 85% in LV-pm-shGR EGFP+ cells, as compared to LV-mm-shGR EGFP+ analyzed in the same way (Figure 4.1 A). This partial knockdown, is comparable to that observed *in vitro* (>70%, see CHAPTER 2), and is consistent with previous *in vivo* observations [360].

GR knockdown leads to accelerated neuronal differentiation of NPCs

As different levels of GCs affect the fate of NPCs during embryogenesis [454] and in the adult brain [123], we first investigated the effect of GR knockdown on neuronal differentiation one week after stereotactic delivery of our lentiviral constructs. We found a significantly increased proportion of EGFP+ cells positive for the mature neuron marker NeuN within the internal layers of the GCL, compared to LV-mm-shGR injected controls (Figure 4.1 H-J). This was accompanied by a concomitant increase in the proportion of EGFP+ cells positive for the immature neuron marker DCX in the same layers (Figure 4.1 K-M). Interestingly, the proportion of EGFP+ cells positive for the neuronal progenitor marker Nestin -exclusively located in the SGZ in both experimental groups- was unaffected by GR knockdown (Figure 4.1 N-P). These results strongly suggest that GR knockdown accelerates neuronal differentiation in newborn cells, without affecting survival of neuronal progenitors in the DG, as judged by the numbers of Nestin+ cells.

→ ***Figure 4.1 Effective GR knockdown in vivo regulates neuronal differentiation.*** *(A to H) Validation of GR knockdown by lentiviral constructs in vivo. Semi-quantification of GR knockdown in EGFP positive cells of the dentate gyrus* ***(A)****. GR expression levels detected by immunohistochemistry in EGFP+ cells within the GCL and SGZ were normalized to expression levels in equal numbers of individual GR+ cells in the CA1 area within the same hippocampal section, negative for EGFP (125 cells per experimental group, * p< 0.0001, unpaired Student's t-test). The effective (LV-PM,* ***B****) or ineffective (LV-MM,* ***E****) lentiviral constructs were delivered by stereotactic injection into the hilus and GR knockdown was analyzed in cells expressing the enhanced green fluorescent protein (EGFP, green) by GR immunohistochemistry (red) 1 week PI (post-injection). Orthogonal projections corresponding to boxed areas in B show a sample cell positive for GR expression* ***(C)*** *and a sample cell negative for GR expression* ***(D)****. Cells with highest GR depletion were always found in the proximity or within the Molecular Layer (ML). Orthogonal projections corresponding to boxed areas in E show two sample cells positive for GR expression (****F, G****) irrespective of their relative positioning within the granule cell layer (GCL) or the sub-granular zone (SGZ). Sample orthogonal projections from confocal z-stack images corresponding to animals injected (1 week PI) with LV-PM* ***(H, K, N)*** *or LV-MM* ***(I, L, O)****, showing EGFP and* ***(H, I)*** *NeuN,* ***(K, L)*** *DCX and* ***(N, O)*** *Nestin co-immunostainings. Distribution plots of EGFP and* ***(J)*** *NeuN,* ***(M)*** *DCX and* ***(P)*** *Nestin double-positive cells within four subdivisions of the GCL (SGZ, GCL1-3; Experimental Procedures). Values represent mean ± SD (n = 5 animals per group); * p< 0.05, unpaired Student's t test. Nestin positive cells were only observed in the SGZ. Scale bars: 10 μm.*

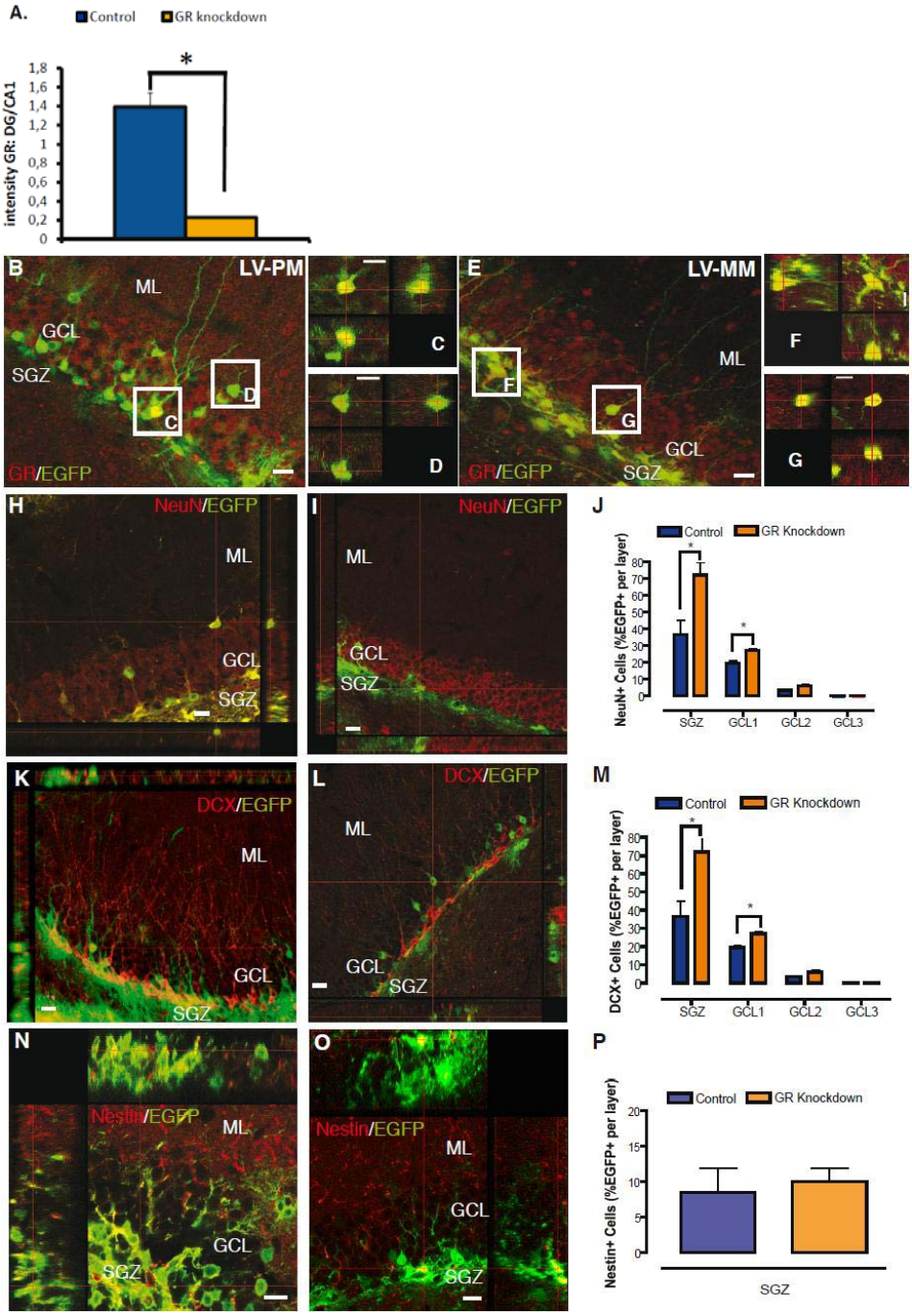
A.
Control
GR knockdown
intensity GR: DG/CA1
B
LV-PM
ML
GCL
SGZ
GR/EGFP
C
D
E
LV-MM
F
G
H
NeuN/EGFP
I
J
Control
GR Knockdown
NeuN+ Cells (%EGFP+ per layer)
SGZ
GCL1
GCL2
GCL3
K
DCX/EGFP
L
M
DCX+ Cells (%EGFP+ per layer)
N
Nestin/EGFP
O
P
Nestin+ Cells (%EGFP+ per layer)

GR knockdown in NPCs leads to an altered dendritic tree and dendritic spine profile

During neuronal differentiation, new granule cells migrate from the sub-granular zone outwards, to the edge of the cell layer [368;455]. This is accompanied by changes in the dendritic arborization of neurons in the DG, with cells in the outer layer showing more dendrites branching from the soma and more complex dendritic arborization than cells in the inner layer [433]. Consistent with these observations we found that GR knockdown induced differential morphological features in EGFP+/ NeuN+ neurons (Figure 4.2 A-B). To characterize these differences, we reconstructed dendritic arborization of individual EGFP+ neurons in the DG. Compared to control animals, EGFP+ neurons in GR knockdown animals consistently showed more complex dendritic arbors (Figure 4.2 C-D).

Consistent with previous observations [433], Sholl analyses demonstrated the existence of two different populations of EGFP+ neurons. We named these populations A and B cells. 'A' cells have simpler dendritic arbors than B cells (Figure 4.2 E-F). Moreover, near the cell body, A cells present a unique primary dendrite with a smooth, a-spiny proximal dendritic domain and a spiny distal dendritic domain, while in B cells both the proximal and distal dendritic domains present abundant spines (Figure 4.2 C-D). Interestingly, the number of B cells was significantly increased in GR knockdown animals, with all B cells located in the most external third of the GCL (Figure 4.2 G). These observations are consistent with a premature progression into neuronal differentiation of newborn neurons in the adult hippocampus after GR knockdown.

The morphological alterations after GR knockdown are likely regulated by GR-responsive genes [219]. In previous work, we have identified a number of genes like BDNF, LIM kinase 1(LIMK-1) and Calcineurin A, that also regulate spine dynamics as GR -responsive [22;456-458]. Therefore, we reasoned that GR could be involved in regulating dendritic spine morphology in newborn neurons of the adult hippocampus. Multiple studies have demonstrated that newborn neurons in the adult hippocampus integrate into pre-existing circuits, receiving fully functional excitatory inputs and forming morphologically mature synapses, which is reflected in the shape of the dendritic spines [95;427;459]. Since mature granule neurons receive the majority of their synaptic input through dendritic spines, their numbers and morphology is indicative of their connectivity within hippocampal circuits [95].

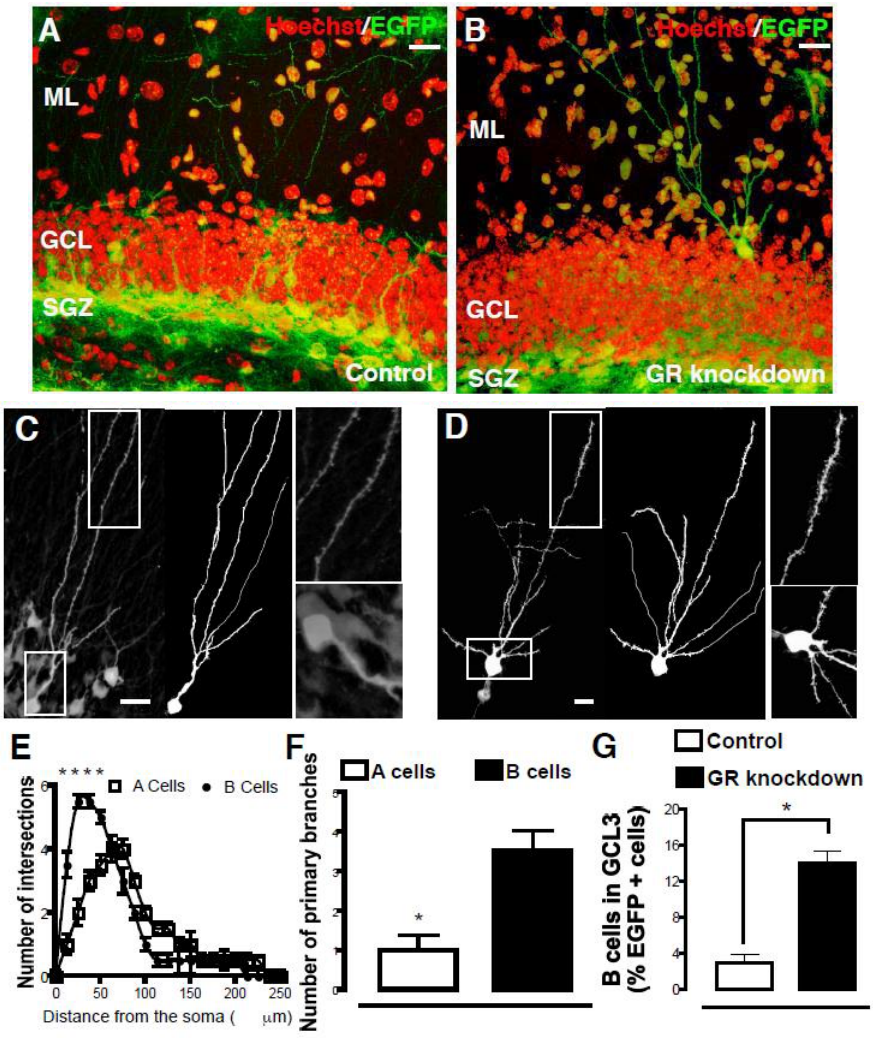

Figure 4.2 GR regulates dendritic morphology of newborn neurons. *Sample confocal images showing denditic morphology of EGFP+ cells and their location within the GCL from animals injected with LV-MM* ***(A)*** *or LV-PM* ***(B).*** *3D confocal reconstruction of somas and dendrites of EGFP+ newborn neurons, obtained 1 week PI (****C****, Control;* ***D****, GR knockdown). Left panels show original images, center panels corresponding 2D projected dendritic trajectories and right panels show details of the distal (top) or proximal (bottom) to soma dendritic domains corresponding to boxed areas in the original image. Panels showing proximal domains were rotated 90 degrees clockwise. Only EGFP+ neurons with obvious dendritic spines were considered for analysis. Scale bar: 10 μm.* ***(E)*** *Sholl analysis of dendritic complexity of EGFP+ neurons 1 week PI. Values represent mean ± SD (n=5 animals per group), * p< 0.05, one-way ANOVA.* ***(F)*** *Dendritic properties of EGFP+ newborn neurons 1 week PI. Values represent mean ± SD (same cells as in E, n=5 animals per group), * p< 0.05, unpaired Student's t-test.* ***(G)*** *Presence of "B" cells (results section) in GCL3 (Experimental Procedures) as percentage of total EGFP+ cells in GCL in control vs. GR knockdown animals. * p< 0.05, unpaired Student's t-test.*

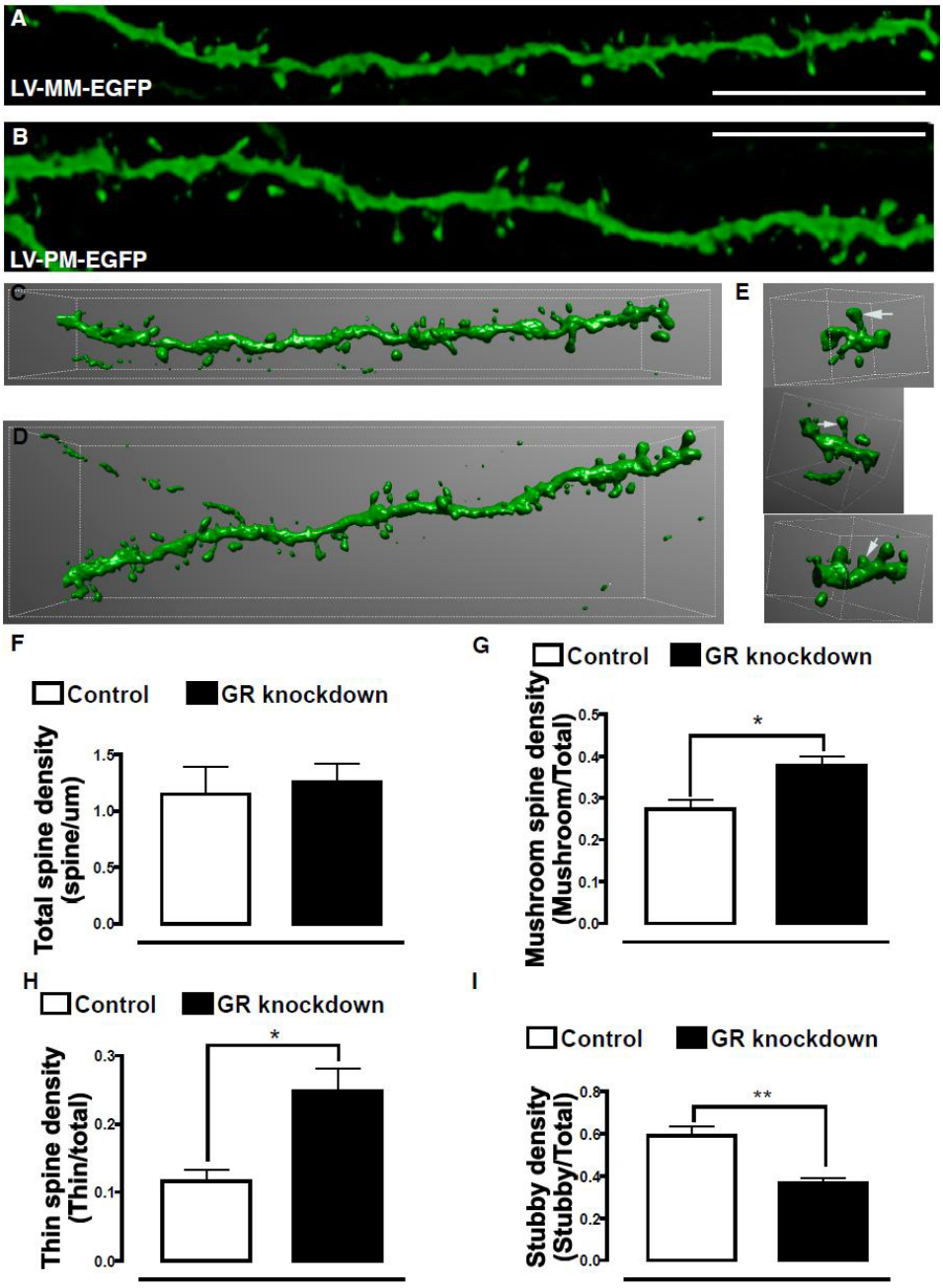

Figure 4.3 GR regulates dendritic spine maturation in newborn neurons. *Sample deconvolved confocal images of spiny dendrites of newborn neurons in* ***(A)*** *Control or* ***(B)*** *GR knockdown animals and their corresponding 3D reconstructions (**C**, Control; **D**, GR knockdown). Scale bar: 10 μm.* ***(E)*** *examples of 3D reconstructions of individual mushroom (top), thin (middle) or stubby (bottom) dendritic spines, indicated by arrows. Spine density measurements corresponding to* ***(F)*** *total,* ***(G)*** *mushroom,* ***(H)*** *thin and* ***(I)*** *stubby shaped spines in Control vs. GR knockdown animals. Values represent mean ± SD (n = 5 animals per group), * p< 0.05, unpaired Student's t-test.*

Recently, we have shown that one week after stereotactic delivery of our lentiviral vector, only a small percentage of EGFP+ cells present in the GCL are positive for the mature neuron marker NeuN and have simple dendritic arbors with dendritic spines, whereas the vast majority of EGFP+ cells are positive for the immature neuron marker DCX, with phenotypes ranging from putative dividing neuronal progenitors to early post-mitotic immature neurons [451]. Therefore, we analyzed the density and shape of dendritic spines from EGFP+/NeuN+ neurons in control and GR knockdown animals with visible spines in the proximal molecular layer (Figure 4.3 A-E). We found no significant difference in total spine density between EGFP+/NeuN+ cells in control and GR-knockdown animals (Figure 4.3 F). The average spine densities that we found are consistent with spine densities previously observed in young newborn hippocampal neurons [95].

Dendritic spines can be categorized into at least three different types based on their morphology: mushroom, thin and stubby [460;461]. From these, stubby (headless) spines are associated with developing neurons while thin and mushroom spines, with increased head size, are more abundant in mature neurons [460;462]. Strikingly, we found a significant increase in the percentage of mushroom and thin spines in EGFP+/NeuN+ cells from GR-knockdown compared to control animals (Figure 4.3 G-H). This increase in mushroom and thin spines was compensated by a significant decrease in stubby spines in GR-knockdown neurons (Figure 4.3 I). Overall, stubby spines were the predominant group of spines (59.2±1.5%) in control animals, while in GR-knockdown animals mushroom spines slightly predominated (37.8±0.7%). Interestingly, although thin spines were the minority group, they constituted the group with the largest fold-change in GR-knockdown neurons (11.7±0.5% and 24.8±1.1 %, 2.11 fold, control vs. GR-knockdown, respectively). These results are again consistent with an accelerated maturation of newborn neurons after GR knockdown in NPCs. Moreover, as the size of spine head may correlate with the efficacy of the corresponding synapse [95], our results strongly suggest a role for GR protein levels in controlling synaptic efficacy in newborn granule neurons of the adult hippocampus.

GR knockdown results in altered mossy fiber boutons

The connectivity of neurons is determined by both afferent input through dendrites and efferent output through axons. As early as 10 days after new granule cells are born in the adult hippocampus they project their axon into the hilus and CA3 areas [95;105;439]. The maturation of dendritic spines of newborn cells has been suggested to be matched with similar development of axonal output [102]. Our observation that GR knockdown animals exhibit increased dendritic spine maturation suggests therefore that axonal synaptic output of newborn cells is also increased. These synaptic contacts, often visible as large mossy fiber synaptic boutons, constitute functional synapses of newborn granule cells with hilar interneurons and CA3 pyramidal neurons. The cross-sectional area of mossy fiber boutons reflects the maturity of the corresponding synapse [102]. Earlier it was reported that a relative increase in GR activation in the hippocampus, e.g. in mineralocorticoid receptor knockout animals [463] or after chronic stress [464], correlates with decreased mossy fiber projections, suggesting a role for corticosteroid receptors in the regulation

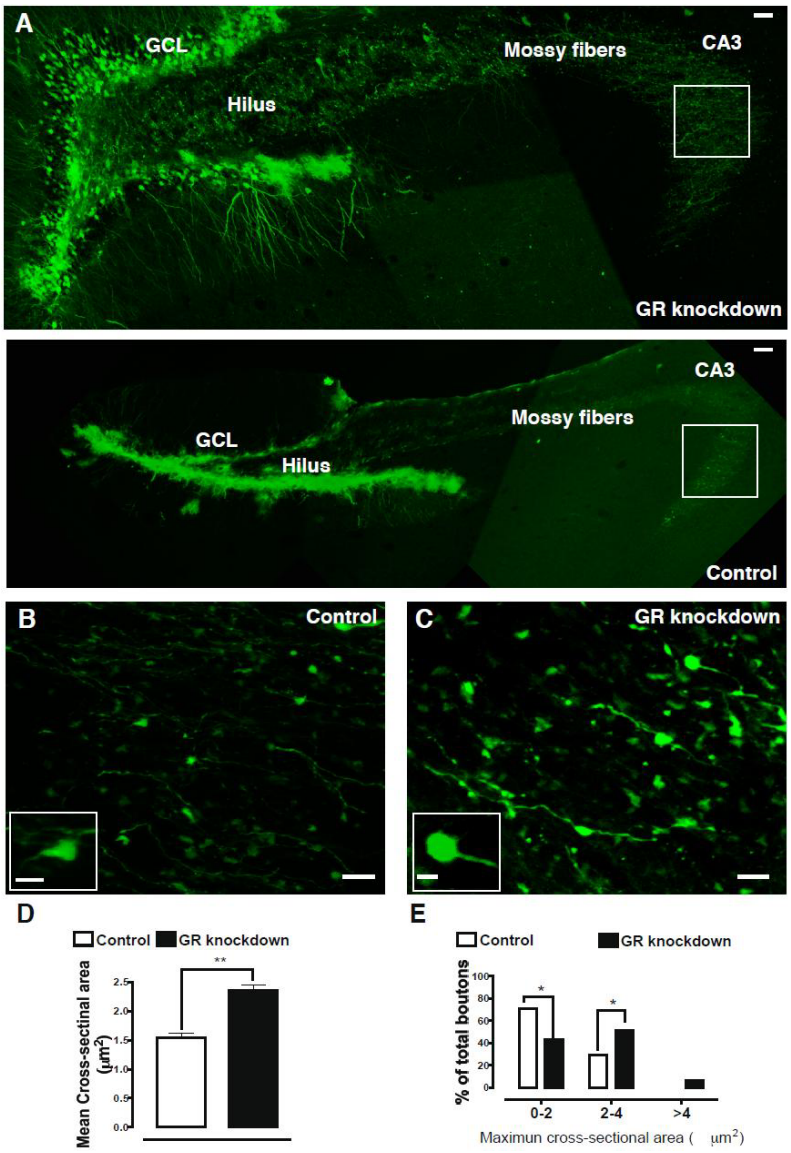

Figure 4.4 GR regulates mossy fiber boutons maturation. (A) *Sample confocal images showing an overview of the hippocampus with a subpopulation of lentivirus-transduced cells in green (EGFP) in GR knockdown (top) or Control (bottom) animals, 1 week PI. Images are compositions of 5-6 individual images obtained at 40X and processed using the automatic Photomerge function of Adobe Photoshop CS2 (Macintosh version). Examples of mossy fiber axons labelled with EGFP in the CA3 corresponding to* ***(B)*** *Control or* ***(C)*** *GR knockdown. Insets show high magnification examples of giant boutons in the CA3. Scale bars: 10 μm (A-C) and 2.5 μm (insets).* ***(D)*** *Cross-sectional area of EGFP+ boutons at the largest section, calculated from 3D reconstructions of original images exemplified in B and C in Control vs. GR knockdown animals.* ***(E)*** *Frequency distribution plot of the size of mossy fiber boutons in Control vs. GR knockdown animals. Giant mossy fiber boutons in CA3 were grouped according to their size, and the percentage of boutons in each size group was calculated. In all cases values represent mean ± SD (n = 5 animals per group); *p< 0.05, unpaired Student's t-test.*

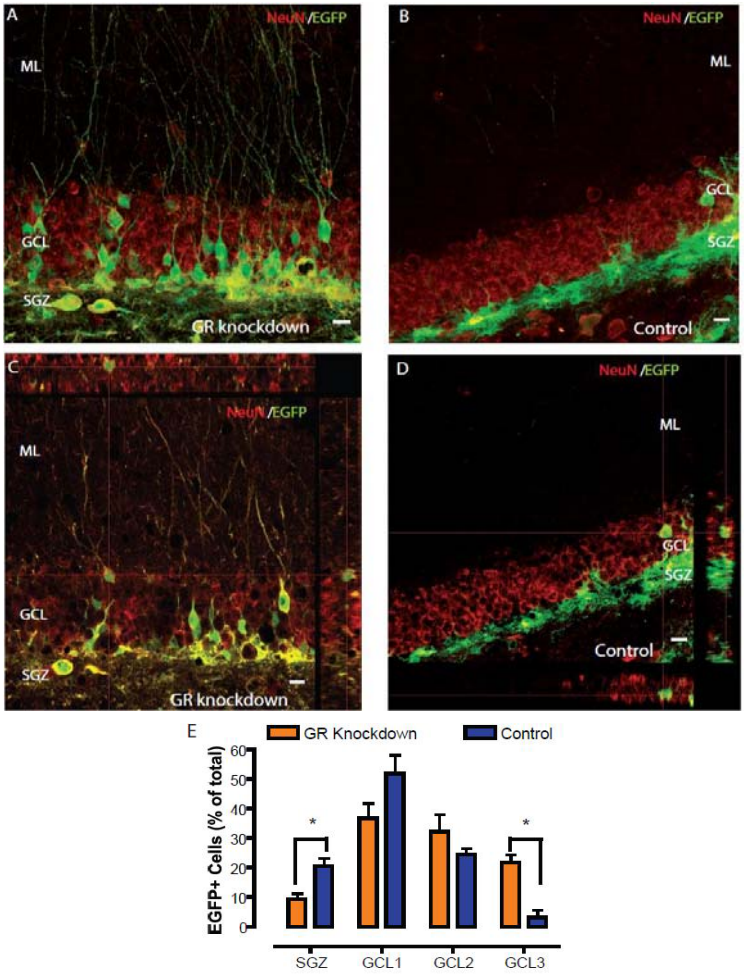

Figure 4.5 GR regulates positioning of newborn neurons within the GCL. *See for legend next page.*

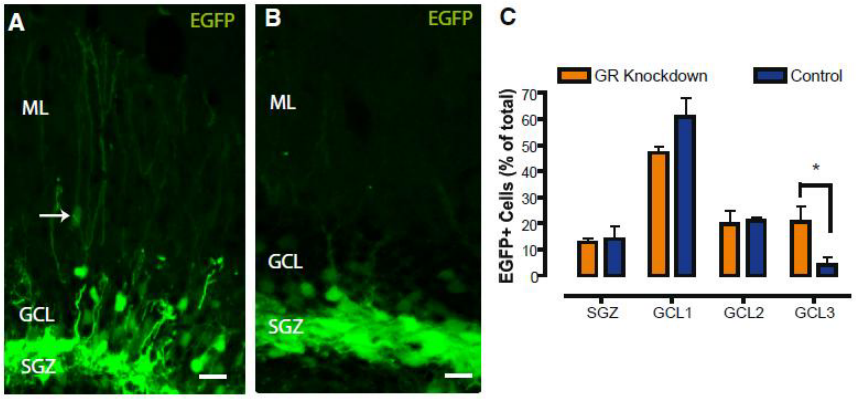

Figure 4.6 GR regulates resting membrane electrophysiological properties of newborn neurons (part 1).

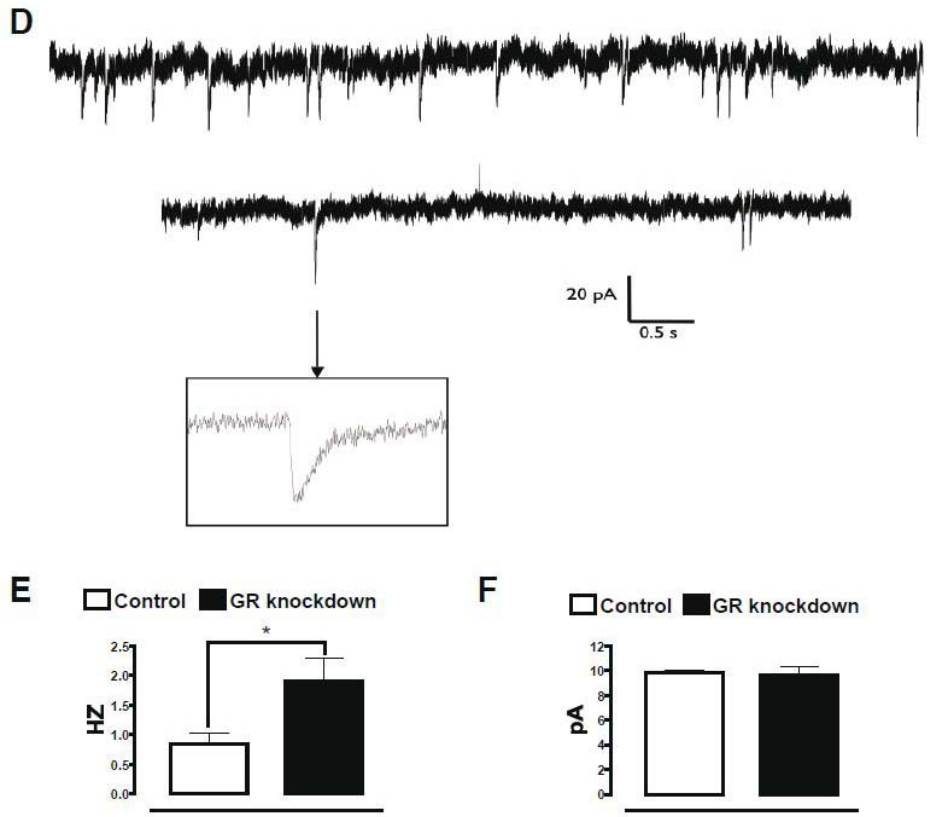

Figure 4.6 GR regulates resting membrane electrophysiological properties of newborn neurons (part 2). *Sample confocal images of EGFP+ (green) immunostaining from (**A**) GR knockdown or (**B**) Control animals 5 weeks PI, showing the persistent mis-location of EGFP+ cells after GR knockdown. The arrow in (**A**) shows a sample EGFP+ cell ectopically located in the ML. (**C**) Bar graphs showing the relative positioning of EGFP+ cells within four subdivisions of the GCL (SGZ, GCL1-3; methods section) normalized to total EGFP+ cell numbers 5 weeks PI in Control vs. GR knockdown animals. Values represent mean ± SD (n = 5 animals per group); * p< 0.05, unpaired Student's t-test. (**D**) Examples of paired mEPSC recordings in GR knockdown (top) or Control (bottom) animals treated with LV-PM (top) or LV-MM (bottom), 5 weeks PI. Inset shows a sample mEPSC. Scale bars represent 0.5s, 20 pA. mEPSC mean frequency (**E**) and amplitude (**F**) in animals in Control vs. GR knockdown animals. Values represent mean ± SD: n= 10 animals per group; * p< 0.05, unpaired Student's t-test.*

← ***Figure 4.5 GR regulates positioning of newborn neurons within the GCL.*** *Sample confocal images of EGFP (green) and NeuN (red) immunostainings in (**A**) GR knockdown or (**B**) Control animals, showing the differential positioning of EGFP+ neurons within the pre-existing granule neurons of the GCL, 1 week PI. Corresponding orthogonal projections (**C**, GR knockdown; **D**, Control) showing examples of EGFP/NeuN double-positive neurons. (**E**) Bar graphs showing the relative positioning of EGFP+ cells within four subdivisions of the GCL (SGZ, GCL1-3; Experimental Procedures) normalized to total EGFP+ cell numbers, 1 week PI. Values represent mean ± SD (n = 5 animals per group); * p< 0.05, unpaired Student's t-test.*

of mossy fiber connectivity. Therefore, we studied the layout of mossy fibers in GR-knockdown animals by analyzing axons and axon terminals in the CA3 area using confocal microscopy.

We found that the mossy fiber boutons in CA3 were substantially larger in one week GR-knockdown animals than those in the control group animals (Figure 4.4 A-C). The mossy fiber boutons in GR-knockdown animals had a significantly larger mean cross-sectional area than those in control animals (Figure 4.4 D, p=0.007; 2.4±0.1μm^2 vs. 1.5±0.1 μm^2 GR-knockdown, n=109, and Control, n=102, respectively. p=0.007). Moreover, a frequency distribution analysis of mossy fiber bouton size showed that in control animals the majority (70.7 %) of the boutons had a cross-sectional area smaller than 2 μm^2, while in GR-knockdown animals the majority (57.2 %) of the boutons had a cross-sectional area larger than 2 μm^2. In contrast, 6.3% of the boutons in GR knockdown animals had a cross-sectional area larger than 4 μm^2, which was not observed in control animals (Figure 4.4 E). These results suggest that, together with those presented in previous sections, GR-knockdown in adult-born granule cells induces a differential connectivity pattern to hippocampal circuits that may result in increased excitability.

GR knockdown leads to altered positioning of adult newborn cells

In our analysis of dendritic arborisation and spine morphology of newborn cells, we noted a marked dispersion of EGFP+ cells within the pre-existing granule cells of the granule cell layer (GCL) 1 week after treatment with LV-pm-shGR, which was nearly absent with LV-mm-shGR. Moreover, EGFP+ cells that retained high GR expression were located in the internal layers of the GCL, while EGFP+ cells with more profound GR knockdown were consistently located in more external layers of the GCL (Figure 4.5 A-D). These results suggest a role for the GR in the accurate positioning of newborn cells within the pre-existing GCL. In line with this are recent findings that excess glucocorticoids retard neuronal migration of NPCs during the cortical development [465]. Therefore, we proceeded by comparing in detail the relative contribution of EGFP+ cells to the pre-existing GCL in groups of animals treated with LV-pm-shGR (GR knockdown) or LV-mm-shGR (control) and their progression into neuronal differentiation (Figure 4.5 E). We found that the proportion of EGFP+ cells located to specific GCL subdivisions, termed SGZ and GCL1-3 from the hilus to the Molecular Layer (Methods section), was significantly different in GR knockdown compared to control animals. The majority of the cells in control animals were located in the inner layers, which is in line with normal migration patterns of adult-born new neurons [76;94]. Strikingly, in GR knockdown animals, the majority of the cells had progressed towards the outer layers, with a significant higher number of EGFP+ cells in GCL3 for GR knockdown animals (Figure 4.5 E). This seemed to be accompanied by a significant reduction of the number of EGFP+ cells in the SGZ. Thus, GR knockdown leads to an altered positioning of adult newborn neurons in the different layers of the DG.

GR knockdown leads to sustained mis-positioning of NPCs and affects basal membrane excitability

To check if 5 weeks of GR knockdown also resulted in mis-positioning of newborn cells we have analysed the location of EGFP+ cells in the different DG layers (Figure 4.6 A-B). For the position of EGFP+ cells in the different layers, time was not significant for both treatment groups. In fact, significantly ($p< 0,05$) higher numbers of EGFP+ cells were found in GLC3 in GR knockdown animals compared to control animals, indicating long-lasting effects of GR knockdown on the formation of hippocampal neo-networks (Figure 4.6 C).

To further test the contribution of newborn cells of GR knockdown animals in hippocampal circuitry we analysed the potential synaptic strength by recording spontaneous miniature excitatory postsynaptic currents (mEPSCs) as a measure of the spontaneous excitatory transmission (Figure 4.6 D), with whole cell voltage clamp (holding potential V_H=-70 mV). EGFP+ cells within the granule cell layer were identified as neurons by the shape and location of their soma and dendritic tree. Consistent with the increased proportion of mature spines, EGFP+ cells in GR-knockdown animals presented a significant ($p=0.03$) increase in the frequency of mEPSCs, as compared to EGFP+ cells in control animals (Figure 4.6 E). The mean frequency of mEPSCs in control EGFP+ cells was highly comparable to that of neighbouring non-EGFP cells. No differences in mEPSC amplitude were detected between GR-knockdown and control EGFP+ cells (Figure 4.6 F) or neighbouring EGFP- cells. Collectively, these data corroborate that GR-knockdown in newborn hippocampal neurons induces drastic increases in basal membrane excitability, thus suggesting their participation in hippocampal circuitry.

DISCUSSION

Here we show that GR protein levels in NPCs are a key determinant for functional integration of adult born granule cells in hippocampal neo-networks. Firstly, GR knockdown leads to an accelerated neuronal differentiation of newborn cells. Secondly, downregulation of GR leads to a significant change in the relative positioning of newborn cells in the external layers of the GCL, or even in the molecular layer. Thirdly, lowering GR protein levels results in a clear shift in spine morphology, with more mature thin and mushroom spines and less immature stubby spines. Fourthly, $EGFP^+$ neurons exhibited increased neuronal activity after GR knockdown, a finding with possible consequences for hippocampal circuitry.

Several studies showed that aberrant GC signalling impairs neurogenesis in the sub-granular zone of the adult dentate gyrus [109;123]. However, the role of the main mediator of glucocorticoids action in NPCs, i.e. the glucocorticoid receptor, remains elusive. This role may be direct or indirect since GRs are expressed in virtually every cell type in the DG, which confounds the interpretation of studies aiming to unravel the contribution of the GR in NPCs using classical transgenesis models. Therefore, we here used lentiviral vectors to specifically knockdown GR in the neurogenic niche of the dentate gyrus [451]. Our data clearly indicate that aberrant GC signalling may target directly the fate of NPCs and that GR, expressed in NPCs, has a key role in proper integration of newborn neurons into existing hippocampal neuronal circuits.

The process of adult hippocampal neurogenesis comprises of several stages: proliferation, survival, migration, neuronal differentiation and functional integration into the hippocampal trisynaptic circuitry. Thus far, stress, and aberrant GC signalling have been mainly associated with antineurogenic effects at the initial stages (reviewed in CHAPTER 1.3.2); cell proliferation [82;137;158;466] and cell survival [92;122]. These stages are mainly associated with quantitative aspects of neurogenesis.

In this study, we have found several lines of evidence that GR is involved in later stages of neurogenesis. GR knockdown in NPCs resulted in accelerated differentiation. In addition, our study revealed morphological alterations in dendritic arborisation, dendritic spines and boutons. Perhaps most importantly, our study showed that GR in NPCs controls correct positioning of NPCs as well a physiological evidence for an aberrant functional integration of NPCs into hippocampal networks. Our results indicate therefore GR knockdown in NPCs might have possible implications for the functioning of the hippocampus. In a study by Herbert and Wong (2006), a first indication for an involvement of GR in later stages of neurogenesis was observed. Systemic injections with high concentrations of GCs, thus activating GR, "discouraged" the acquisition of neuronal fate in a time-dependent fashion [123]. GCs given during the post-mitotic interval were shown to reduce the differentiation of newly formed cells into mature neurons as determined 1 and 4 weeks after treatment. Together, these data imply that GR's are not only involved in regulating the number of newborn neurons (referred to as "quantitative" aspects), but also in controlling several aspects of neuronal development, such as spine and bouton formation of newborn neurons (referred to as "qualitative" aspects).

How to explain these qualitative aspects of neurogenesis upon GR knockdown? One possible explanation is underlying the molecular function of GR as a transcription factor. This implies a more or less direct GR-mediated effect on differentiation, migration and integration. However, the signalling pathway downstream of the GR is not yet resolved. A first indication as to the nature of these signals comes from a study showing that the phenotype of newborn cells after knockdown of Disrupted-In-Schizophrenia 1 (DISC1; [368], a gene of which genetic variants have been implicated in the pathogenesis of schizophrenia [467], is strikingly reminiscent of what we observed after GR knockdown. Similarly as in our study, DISC1 knockdown in NPCs leads to enhanced excitability, accelerated neuronal maturation and synapse formation and to aberrant integration of newborn cells into hippocampal neo-networks. This similarity in phenotype after GR and DISC1 knockdown suggests that both proteins may be involved in the same signalling cascade directing newborn granule cells to their destination. One such potential converging pathway might be GSK3beta, a kinase involved in the control of cell proliferation and direct target of the anti-depressant lithium, as both both DISC1 and GR have been shown to control GSK3beta activity in neuronal progenitor cells [56;468].

A second indication can be inferred from the observation that GR knockdown leads to a significant increase in the frequencies of spontaneous mEPSCs as well as in the numbers of mature-type mushroom and thin spines, indicative of increased glutamatergic neurotransmission [469]. This may be the result of overall acceleration of neuronal differentiation by increased neuronal activity

caused by GR knockdown. Neuronal activity is a major determinant for the maturation rate of newborn cells. Alternatively or in combination with other factors, the GR may control more directly synapse formation and glutamatergic neurotransmission. Indeed, we have reported that the expression of several important components affecting spine formation, such as BDNF [456], LimK-1 and calcineurin A [22], is controlled by GRs at the genomic level. More recently, synaptic GR-dependent glutamate receptor clustering has been reported by us and others [470;471]. In addition, GRs are known to alter glutamate signalling [89;132-136]. Also, a number of excitatory stimuli are known to be influenced by GR-mediated transcriptional regulation. Excitatory stimuli of NPCs are thought to release BDNF and also activate glutamatergic signalling via NMDA receptors, calcium entry, and activation of transcription factors like CREB and AP-1 [64;472-476]. Activated GR is well-known to dampen these excitatory stimuli, for example by downregulation of BDNF [456;477] or by repression of AP-1 and cAMP signalling [478-480]. However, the signalling pathways downstream of GR are a matter requesting further investigations.

Either way, our data indicate a crucial role for appropriate GR expression levels in NPCs for progression of neuronal differentiation and functional integration into existing networks. The question therefore arises to what extent endogenous factors affect GR expression. Recently we showed that GR protein levels are down-regulated by microRNA-124 [59], a non-coding RNA that is endogenously highly expressed specifically in neuronal cells. Interestingly, recent *in vivo* experiments identified microRNA-124 as a master switch that turns on a neuronal differentiation program in neuronal progenitor cells [61] suggesting that reduced GR protein levels are necessary to keep neuronal differentiation within physiological range, a notion that is in line with our data. Equally interesting, several risk factors for the pathogenesis of psychiatric disorders have been shown to result in reduced GR protein levels. To illustrate, decreased maternal care in early life in rats, a rodent model for depression, reduces GR protein levels in the hippocampus [273]; chronic stress, a major risk factor for several psychiatric disorders, is associated with reduced GR protein and mRNA levels in the hippocampus [51;302;481] and aging impairs negative feedback action of glucocorticoids on the HPA-axis that is associated by reduced hippocampal GR protein levels [482]. Extrapolating, our data indicate that reduced GR protein levels under these circumstances can impair hippocampal function by re-organizing hippocampal neo-networks.

In conclusion, we have demonstrated a crucial role for GR expression levels in migration, differentiation and integration of newborn granule cells into hippocampal networks. As the GR is a target for stress-induced elevation in glucocorticoids and for a broad range of pharmacological steroid-based agents, our data suggest that these factors may affect correct integration of newborn cells with possible consequences for neuroplasticity and hippocampal function.